Silencing CDC25A inhibits the proliferation of liver cancer cells by downregulating IL-6 *in vitro* and *in vivo*

SI CHEN[*], YANPING TANG[*], CHUN YANG, KEZHI LI, XIAOQING HUANG and JI CAO

Department of Research, Affiliated Tumor Hospital of Guangxi Medical University, Nanning, Guangxi 530021, P.R. China

Abstract. Cell division cycle 25A (CDC25A) is a core regulator of the cell cycle that has a dual-specific phosphatase activity, which is closely associated with the occurrence and development of a tumor, and is overexpressed in liver cancer. However, the molecular mechanism of CDC25A in the development of liver cancer remains unclear. The purpose of the present study was to further investigate the effect of CDC25A on cell proliferation *in vitro* and *in vivo* and to investigate whether an interaction exists between CDC25A and interleukin (IL)-6 in liver cancer. An Affymetrix human gene expression profiling chip screened differentially expressed genes in HepG2 cells with silenced CDC25A and the IL-6 signaling pathway was revealed to be significantly inhibited (P<0.05). In the present study, the effects of CDC25A on cell proliferation and migration were analyzed using cell cycle, MTT and Transwell assays. Reverse transcription-quantitative PCR, western blot and immunohistochemistry analyses confirmed that silencing the CDC25A gene downregulated the expression of IL-6 in HepG2 cells and the mRNA and protein expression of IL-1β, mitogen-activated protein kinase kinase kinase 14 (NIK) and nuclear factor-κB (NF-κB), which are regulatory molecules upstream of IL-6. In addition, silencing CDC25A by short hairpin RNA inhibited the development of liver cancer xenograft tumor types in nude mice, and decreased the expression of IL-1β, NIK, NF-κB and IL-6 in xenograft tumor types. In conclusion, silencing CDC25A significantly inhibited the proliferation of liver cancer cells *in vitro* and *in vivo*, potentially via an interaction with IL-6 through the downregulation of the IL-1β/NIK/NF-κB signaling axis.

Correspondence to: Professor Ji Cao, Department of Research, Affiliated Tumor Hospital of Guangxi Medical University, 71 Hedi Road, Nanning, Guangxi 530021, P.R. China
E-mail: caoji1973@sina.com

[*]Contributed equally

Introduction

Liver cancer is a malignant tumor type that seriously endangers human life and health, and its morbidity and mortality rates continue to rise faster compared with those of other cancer types (1). China is a high-risk area for liver cancer, accounting for ~50% of new patients and liver cancer-associated mortalities globally each year (2). The occurrence and development of liver cancer are known to utilize a complex evolutionary process involving the accumulation of multiple factors, stages and gene variations (3). Identifying the genes that serve key functions in the development of liver cancer and the associated molecular mechanisms are prerequisites for the treatment of liver cancer. To identify the key genes affecting the development of liver cancer, a previous study proposed a research strategy based on the cross-species screening of early-stage disease, and CDC25A was revealed to be highly expressed in liver cancer (4).

As an important member of the CDC25 family, CDC25A is a bispecific protein phosphatase that hydrolyses tyrosine and serine/threonine residues for dephosphorylation (5). CDC25A activates the cyclin-cyclin-dependent kinase complex, which promotes the transition of the G1/S and G2/M phases and is an important target for DNA damage response (6,7). CDC25A, which has the characteristics of a proto-oncogene, is known to be highly expressed in various malignant tumor types, including lung cancer (8), breast cancer (9) and esophageal cancer (10), and is closely associated with poor patient prognosis. To further investigate the molecular mechanism of CDC25A in liver cancer, an Affymetrix human gene expression profiling chip was used to analyze the differentially expressed genes in HepG2 cells with the CDC25A gene silenced. Based on ingenuity pathway analysis, signaling pathways were revealed to be enriched among the genes with significant differential expression, and the interleukin (IL)-6 signaling pathway was revealed to be significantly inhibited.

IL-6 is a cytokine produced by various cells and serves important functions in information transmittance, immune cell activation and regulation, T and B cell activation, proliferation and differentiation and inflammatory responses (11). Previously, one study demonstrated that IL-6 is closely associated with the occurrence, development and metastasis of various malignant tumor types, which may be associated with its antiapoptotic and proangiogenic effects (12). IL-6 has been confirmed to affect liver cancer proliferation and serves an important function in the development and recurrence of

liver cancer (13). IL-6 is a major inducer of signal transducer and activator of transcription 3 (STAT3) phosphorylation and activation. IL-6 binds to glycoprotein 130 and induces Janus kinase phosphorylation, which results in the phosphorylation of Tyr705 in STAT3, the promotion of STAT3 binding to DNA and the activation of certain genes downstream of STAT3 to promote the development of liver cancer (14,15).

Nuclear factor-κB (NF-κB), an important transcriptional regulator, participating in the bodily inflammatory response, the immune response, cell apoptosis, differentiation, regeneration and other important physiological and pathological processes. NF-κB is an important molecular marker linking the inflammatory response with tumors (16,17). Activated NF-κβ is involved in cell proliferation, increases the expression of inflammation-associated factors, inhibits apoptosis and promotes the malignant transformation, invasion and metastasis of a tumor (18,19). One study confirmed that NF-κB serves an important function in the induction of IL-6 expression (20). Interestingly, CDC25A has been revealed to positively regulate NF-κB, inhibit apoptosis and promote tumor cell survival (21). Therefore, the present study hypothesized that CDC25A may regulate the expression of IL-6 through the NF-κB gene, further affecting the occurrence and development of liver cancer.

The present study investigated the molecular mechanism of CDC25A in the development of liver cancer, and the results may provide a novel theoretical basis for the treatment of liver cancer based on the utilization of CDC25A as a target.

Materials and methods

Cell culture. HepG2 cells (human liver cancer cell line) were purchased from the Shanghai Cell Biology Institute and cultured in RPMI-1640 medium (Gibco; Thermo Fisher Scientific, Inc.) supplemented with 10% fetal bovine serum (FBS; Gibco; Thermo Fisher Scientific, Inc.) at 37°C in a 5% CO_2 incubator.

Cell transfection. Lentiviral particles [LV-short hairpin RNA (shRNA)-CDC25A] for silencing the CDC25A gene and negative control empty lentiviral particles (LV-shRNA-NC) were obtained from Shanghai GeneChem Co., Ltd., and the lentiviral interference sequences were 5'-CATGCACCA CGAGGACTTT-3' and 5'-TTCTCCGAACGTGTCACGT-3', respectively. The two lentiviruses contained a green fluorescent protein (GFP) marker. Cells were divided into the following three groups: LV-shRNA-CDC25A-transfected cells (CDC25A-shRNA group), LV-shRNA-NC-transfected cells (CDC25A-NC group) and untransfected cells (control group). There were 3 replicate wells per group. Cells in the logarithmic growth phase were plated into 6-well plates at a density of $5x10^4$/ml in 2 ml per well, containing the virus particles, polybrene (a final concentration of 5 g/ml; Shanghai GeneChem Co., Ltd.) and the enhanced infection solution (ENi.s). Once the cells reached 20-30% confluence, they were transfected at a multiplicity of infection of 30. The GFP positive expression rate was observed at 24, 48 and 72 h after infection under a fluorescence inverted microscope (Olympus Corporation). The cell transfection efficiencies were detected by RT-qPCR and western blot analyses.

Cell proliferation assay. MTT Cell Proliferation and Cytotoxicity Assay kit (Beijing Solarbio Science & Technology Co., Ltd., Beijing, China) was used to detect cell proliferation, according to the manufacturers protocol. The cell suspension was seeded in a 96-well plate at a density of $2x10^4$/ml (100 μl total). Each group was placed in 5 wells. The cells were cultured at 37°C in a 5% CO_2 incubator. On days 1, 2, 3, 4 and 5, cells were incubated with 10 μl 5 mg/ml MTT solution for 4 h at 37°C. Next, 100 μl dimethyl sulfoxide was added to each well, and the plates were shaken for 5-10 min. The absorbance at 490 nm was analyzed using a microplate reader (Thermo Fisher Scientific, Inc.) to plot the growth curve.

Cell migration assay. Cell migration was conducted in a Transwell chamber. Subsequent to resuspending the cells in RPMI-1640 medium, 100 μl cell suspension ($1x10^5$ cells) was added to the upper chamber, and 30% FBS in RPMI-1640 medium was added to the lower chamber. The plate was placed at 37°C in a 5% CO_2 incubator for 24 h. Next, the cells that did not pass through the polycarbonate membrane were removed with a cotton swab, and the cells on the lower surface were stained with 1% Giemsa (Beijing Solarbio Science & Technology Co., Ltd.) at room temperature for 20 min, rinsed with phosphate buffered saline (PBS), air-dried, and counted under an inverted microscope (Olympus Corporation).

Cell cycle assay. Single-cell suspensions from the CDC25A-shRNA CDC25A-NC and control groups ($1x10^6$ cells/ml in ice-cold PBS) were prepared, and then subsequently fixed with 70% ethanol at 4°C for 2 h. Subsequent to treatment with RNase A (10 μg/ml) for 30 min at 37°C, the cells were resuspended in 500 μl propidium iodide solution. Cell cycle distribution was analyzed by a FACS Calibur flow cytometer (BD Biosciences).

Gene chip screening. Gene chip screening was performed as described in our previous study (22).

Construction of the liver cancer xenograft model. A total of 30 female BALB/c nude mice (weighing 18-24 g and aged 4-6 weeks) were purchased from Beijing Vital River Laboratory Animal Technology Co., Ltd. (Beijing, China). The study was ethically approved and supervised by the Ethics Committee of Guangxi Medical University Affiliated Tumor Hospital (approval no. LW2019045). The mice were housed in a specific pathogen-free animal room at 22-24°C with a humidity of 55-70% and a 12/12 h light/dark cycle at the Experimental Animal Center of Guangxi Medical University, and all animals were provided *ad libitum* access to standard laboratory feed and water. Their health and behavior were monitored every 5 days. The nude mice were randomly divided into the following three groups (n=10): The knockdown (KD), NC and control groups. The KD group was HepG2 cells transfected with LV-shRNA-CDC25A, the NC group was HepG2 cells transfected with LV-shRNA-NC, and the control group was untreated cells. All cells were resuspended at a concentration of $1x10^7$/ml, and cell suspensions (200 μl) were subcutaneously injected into the right axilla (0.5 cm) of the nude mice. The tumor volume was observed and recorded every 7 days. When the animals exhibited a loss

of appetite and inability to eat, clinical symptoms of severe loss of organ function or when the tumor was observed to be ulcerated, infected or necrotic, the animals were euthanized. Following 35 days, the nude mice were euthanized by cervical dislocation, then the breathing, corneal reflex and heartbeat were observed to determine euthanasia. The criteria for verifying animal mortality are no breathing, no heartbeat and no corneal reflex. The liver cancer xenograft tumors were then harvested. The tumor volume formula used was as follows: Volume (mm^3)=width^2 (mm^2) x length(mm)/2.

Hematoxylin and eosin (H&E) staining. Xenograft tumors were fixed with 4% paraformaldehyde at room temperature for 24 h, embedded in paraffin and serially sectioned at a thickness of 5 μm. The sections were dewaxed and stained with H&E using a staining kit (cat. no. c0105; Beyotime Institute of Biotechnology), and visualized using a phase contrast microscope (Olympus Corporation) at a magnification of x200.

RNA extraction and RT-qPCR. Total RNA was extracted from the liver cancer cells and xenograft tumors using TRIzol (Invitrogen; Thermo Fisher Scientific, Inc.), and cDNA was synthesized using the PrimeScript RT Reagent kit (Takara Bio, Inc.), according to the manufacturer's protocol. qPCR was performed with a qTOWER^{3}G PCR instrument (Analytik Jena AG) and SYBR® Premix Ex Taq™ (Takara Bio, Inc.), according to the manufacturer's protocol. The reaction conditions were as follows: Predenaturation at 95°C for 30 sec, denaturation at 95°C for 5 sec and annealing at 60°C for 30 sec for a total of 40 cycles. The results obtained were analyzed using the $2^{-\Delta\Delta Cq}$ method (23). The primers used were as follows: CDC25A forward, 5'-TTCCTCTTT TTACACCCCAGTCA-3' and reverse, 5'-TCGGTTGTCAAG GTTTGTAGTTC-3'; IL-6 forward, 5'-ACTCACCTCTTC AGAACGAATTG-3' and reverse, 5'-CCATCTTTGGAA GGTTCAGGTTG-3'; IL-1β forward, 5'-GCCAGTGAAATG ATGGCTTATT-3' and reverse, 5'-AGGAGCACTTCATCT GTTTAGG-3'; NIK forward, 5'-AGGAGAAGACGCCGCCA CTG-3' and reverse, 5'-TGCCTCGGAGCCTTCCTTGG-3'; NF-κB forward, 5'-CCCACGAGCTTGTAGGAAAGG-3' and reverse, 5'-GGATTCCCAGGTTCTGGAAAC-3'; GAPDH forward, 5'-TGACTTCAACAGCGACACCCA-3' and reverse, 5'-CACCCTGTTGCTGTAGCCAAA-3'.

Western blot analysis. The cells and xenograft tumors were lysed with RIPA-phenylmethylsulfonyl fluoride buffer (cat. no. P0013K; Beyotime Institute of Biotechnology) to extract the total protein, and the protein concentration was determined using the BCA method. Protein buffer was added to the samples and denatured at 100°C. Each well was loaded with 50 μg proteins. Then, the samples were electrophoresed on a 10% SDS-PAGE gel at 60V for 150 min, transferred to a 0.22-μm-pore size polyvinyline difluoride (PVDF) membrane, and blocked with 5% skimmed milk at room temperature for 2 h. The membranes were washed and incubated while shaking overnight at 4°C with anti- CDC25A (1:5,000; rabbit; cat. no. ab202485; Abcam), anti-IL-6 (1:1,000; rabbit; cat. no. ab233706; Abcam), anti-IL-1β (1:1,500; rabbit; cat. no. ab2105; Abcam), anti-NIK (1:1,000; rabbit; cat. no. ab155583; Abcam), anti-NF-κB (1:1,000; rabbit; cat. no. ab32536; Abcam), anti-β-actin (1:1,000;

rabbit; cat. no. ab8227; Abcam) and anti-GAPDH (1:1,000; mouse; cat. no. ab8245) antibodies. Subsequent to washing, the membranes were incubated with the appropriate horseradish peroxidase-conjugated secondary antibody (1:1,000; goat anti-rabbit or anti-mouse antibody; cat. nos. A0208 and A0216, respectively; Beyotime Institute of Biotechnology) for 1 h at room temperature. The PVDF membranes were scanned with an enhanced chemiluminescence detection system ChemiDoc MP (Bio-Rad Laboratories, Inc.) and the densitometry was performed using Image Lab software (version 3.0; Bio-Rad Laboratories, Inc.).

Immunohistochemistry. The sections at a thickness of 5 μm were dewaxed, immersed in sodium citrate buffer, incubated at 100°C for 2 min in an autoclave, and then rinsed 3 times with PBS to retrieve the antigens. Then, the sections were placed in 3% H_2O_2 and incubated at room temperature for 25 min in the dark to block the endogenous peroxide. The sections were sequentially incubated overnight with rabbit anti-human CDC25A (1:2,000; cat. no. GB11283; Wuhan Servicebio Technology Co., Ltd.) and rabbit anti-human IL-6 (1:600; cat. no. GB11117; Wuhan Servicebio Technology Co., Ltd.) antibodies at 4°C, and then with a goat anti-rabbit immunoglobulin G solution (1:200; cat. no. G23303; Wuhan Servicebio Technology Co., Ltd.) for 50 min at room temperature. The immunocomplexes were visualized using 3,3'-diaminobenzidine and a light microscope (Olympus Corporation) at a magnification of x200. Two blinded pathologists independently assessed all specimens. The staining intensity was scored as follows: 0 (negative); 1 (weak); 2 (moderate); and 3 (strong). The positive range scores were defined as follows: 0 (0-20%); 1 (21-50%); 2 (51-80%); and 3 (81-100%). The final score was obtained by multiplying the intensity score and the positive range score, and a score ^{3}4 was regarded as high expression.

Statistical analysis. Analyses were performed using SPSS 19.0 statistical software (IBM Corp.). Differences among the CDC25A-shRNA, CDC25A-NC and control groups or among the KD, NC and control groups were analyzed using one-way analysis of variance followed by Student-Newman-Keuls. Correlational analysis was performed with Pearson's correlation coefficient. Measurement data are expressed as the mean ± standard deviation. $P < 0.05$ was considered to indicate a statistically significant difference.

Results

Efficiency of lentiviral infection in HepG2 cells. The expression of GFP was detected after 48 h. Following transfection, the mRNA and protein expression levels of CDC25A in the CDC25A-shRNA group were significantly lower compared with those in the CDC25A-NC and control groups ($P < 0.05$; Fig. 1A and B).

Effect of silencing CDC25A on liver cancer cell growth. The effect of silencing CDC25A on the growth of HepG2 cells was confirmed by an MTT assay, revealing that the proliferation of HepG2 cells was significantly decreased in LV-shRNA-CDC25A transfected cells compared with the CDC25A-NC and control groups ($P < 0.05$; Fig. 1C).
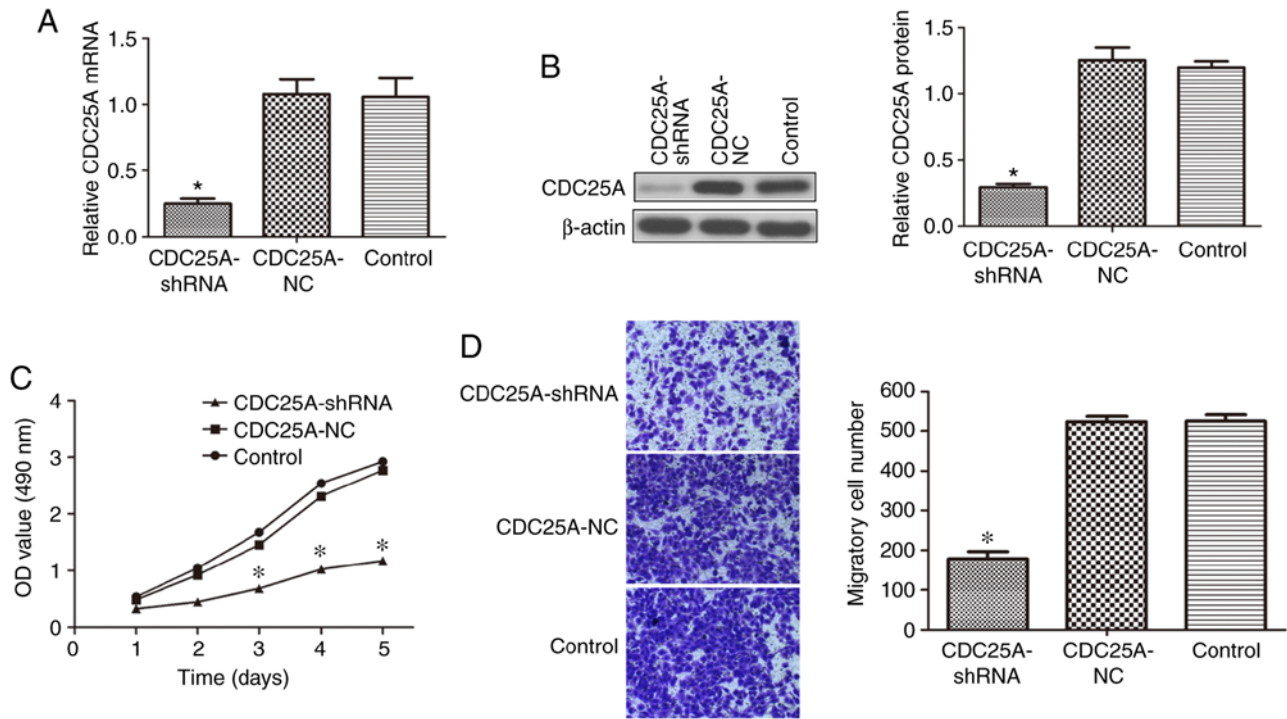
Figure 1. Verification of RNA interference targeting of CDC25A by western blot and reverse transcription-quantitative PCR analyses, and the modulation of CDC25A affects liver cancer proliferation and migration. (A) mRNA and (B) protein expression levels of CDC25A in the CDC25A-shRNA, CDC25A-NC and control groups. (C) Cell proliferation and (D) migration were assessed by the MTT and Transwell assays, respectively. *P<0.05 vs. the CDC25A-NC or control group. CDC25A, cell division cycle 25A; shRNA, short hairpin RNA; NC, negative control; OD, optical density.

Effect of silencing CDC25A on liver cancer cells migration. Migration experiments revealed that significantly fewer cells passed through the membrane in the CDC25A-shRNA group compared with in the CDC25A-NC and control groups (P<0.05; Fig. 1D), and no significant difference was observed between the CDC25A-NC and control groups.

Effect of silencing CDC25A on liver cancer cell cycle. As presented in Fig. 2A and B, the percentage of cells in the G1 phase was significantly increased, accompanied by a significant decrease in S and G2 phases in the CDC25A-shRNA group in comparison with the CDC25A-NC and control groups (P<0.05).

Effect of silencing CDC25A on IL6 expression in HepG2 cells. The differentially expressed genes in HepG2 cells in which the CDC25A gene was silenced mainly involved interferon signaling, the phosphoinositide-3-kinase/protein kinase B signaling pathway, the IL-6 signaling pathway, the P53 signaling pathway and the cell cycle pathway (Fig. 3A), and the IL-6 signaling pathway exhibited the most significant inhibition. These results were verified by RT-qPCR and western blot analyses. As presented in Fig. 3B and C, subsequent to silencing the CDC25A gene, the mRNA and protein expression levels of IL-6 in the CDC25A-shRNA group were significantly lower compared with those in the CDC25A-NC and control groups (P<0.05). These results suggest that CDC25A may affect the expression of IL-6 in HepG2 cells.

Effect of silencing CDC25A on the IL-1β/NIK/NF-κB signaling axis in HepG2 cells. Gene chip screening was performed as described in our previous study (22). The differentially

expressed genes in HepG2 cells with the CDC25A gene silenced revealed that the expression of IL-1β, NIK and NF-κB, which are IL-6 pathway-associated genes, were significantly downregulated (P<0.001; Table I). RT-qPCR analysis revealed that the mRNA expression levels of IL-1β, NIK and NF-κB in the CDC25A-shRNA group were significantly lower compared with those in the CDC25A-NC and control groups (P<0.05). In addition, similar results were obtained regarding protein expression levels (P<0.05; Fig. 3D and E).

Effect of silencing the CDC25A gene on liver cancer xenograft growth. On the seventh day following inoculation, transplanted tumor masses appeared in the nude mice at all inoculation sites. The width and length of each xenograft tumor were measured every 7 days, the tumor volume was calculated and the growth curve was plotted. On the 35th day, the nude mice were sacrificed (Fig. 4A) and the xenograft tumors were harvested (Fig. 4B). As presented in Fig. 4C, the tumor volume in the KD group was significantly smaller compared with that in the NC or control group from day 21 onwards (P<0.05). Correspondingly, the tumor weight in the KD group was significantly decreased (P<0.05; Fig. 4D). Finally, Fig. 4E presents the results of the H&E staining and shows the xenografts were liver cancer tissues, indicating that the liver cancer xenograft models were successfully constructed. These results indicate that silencing the CDC25A gene may inhibit the growth of liver cancer xenografts.

CDC25A affects liver cancer growth by targeting IL-6 through the IL-1β/NIK/NF-κB signaling axis. The expression levels of CDC25A and IL6 pathway-associated molecules
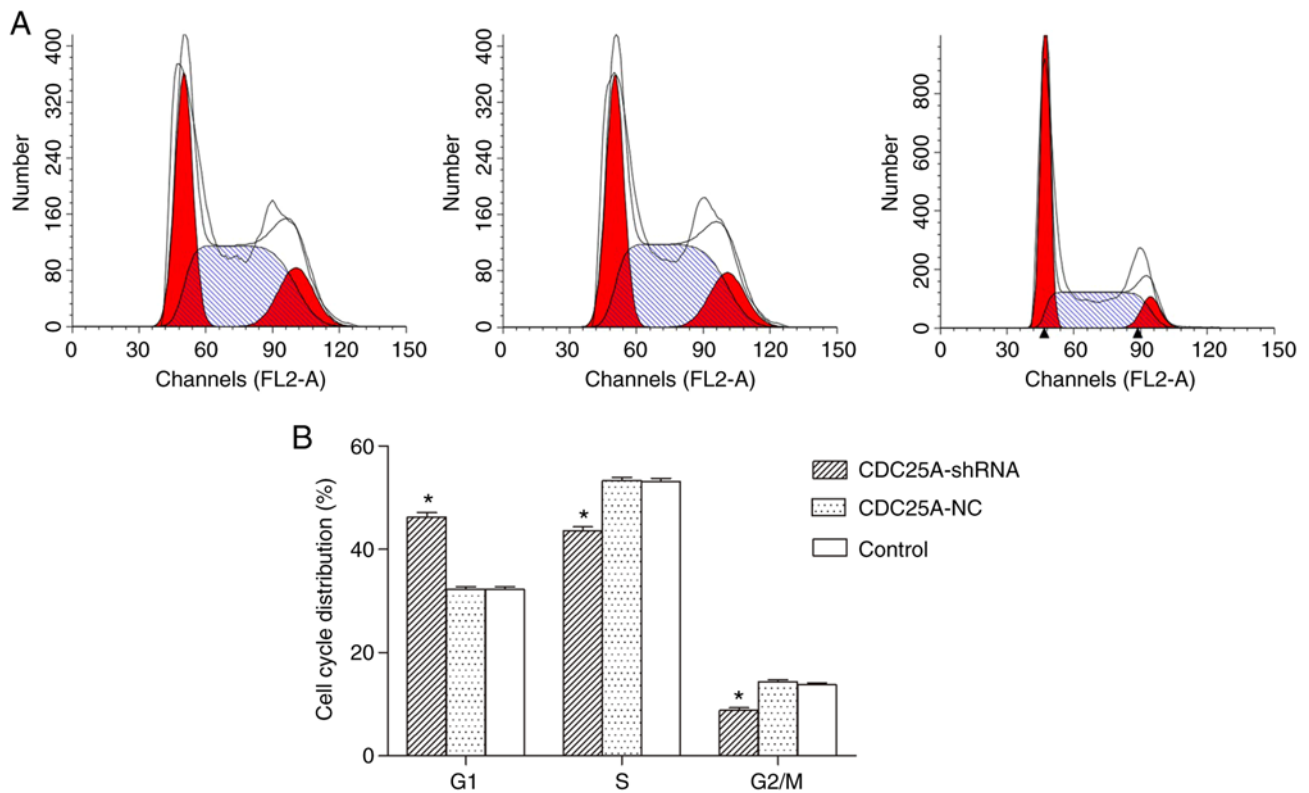
Figure 2. Effects of CDC25A on the HepG2 cell cycle. (A) Cell cycles in the CDC25A-shRNA, CDC25A-NC and control groups were detected using flow cytometry. (B) Distribution of cells in the G1, S and G2/M phases. *P<0.05 vs. the CDC25A-NC or control group. CDC25A, cell division cycle 25A; shRNA, short hairpin RNA; NC, negative control.

(including IL-1β, NIK, NF-κB and IL-6) in the liver cancer xenografts were evaluated by RT-qPCR, western blot analysis and immunohistochemistry. As presented in Fig. 5A and B, the mRNA and protein expression levels of CDC25A and IL-6 were significantly reduced in the KD group compared with the NC or control groups (P<0.05). Further immunohistochemistry analysis revealed that the CDC25A and IL-6 proteins were strongly expressed in the NC and control groups, but their expression levels were lower in the KD group (Fig. 5C). A significant positive correlation was observed between the expression levels of CDC25A and IL-6 in the xenograft tissue samples (R=0.669, P<0.05; data not shown). The mRNA and protein expression levels of IL-1β, NIK and NF-κB in the KD group were significantly lower compared with those in the NC or control group (P<0.05; Fig. 6A-C). These results indicate that CDC25A overexpression in liver cancer may positively regulate IL6 expression by regulating the IL-1β/NIK/NF-κB signaling axis, thereby promoting the growth of liver cancer.

Discussion

CDC25A is a bispecific protein phosphatase consisting of 524 amino acid residues that contains an N-terminal regulatory domain and a C-terminal catalytic domain (24). CDC25A has been revealed to promote cell cycle progression, and the overexpression of CDC25A causes abnormal cell cycle regulation and results in tumorigenesis (25). In addition, previous studies have revealed that CDC25A serves key functions in apoptosis, cell metabolism and tumor cell metastasis (4,26). Overexpressed CDC25A may interact with tumor-associated

factors including mitogen-activated protein kinase kinase kinase 5, NF-κB, STAT3, NIMA related kinase 11, pyruvate kinase M1/2 and forkhead box O1 to promote tumor progression (27-29). CDC25A is overexpressed in liver cancer (30), which is positively associated with clinicopathological parameters including portal vein thrombosis, extrahepatic metastasis and tumor differentiation in patients with liver cancer (31).

In the present study, lentiviral-mediated shRNA transfection was used to silence the expression of CDC25A in HepG2 cells, and the treated cells were inoculated subcutaneously into nude mice. Silencing the CDC25A gene significantly inhibited the growth of the xenograft tumors (P<0.05), indicating that CDC25A is a key gene in the development of liver cancer. Xu et al (32) produced a study that used CDC25A antisense to inhibit CDC25A in liver cancer cells, and revealed that cell growth, invasion and cell cycle were inhibited, which was consistent with the results of the present study.

IL-6 is a multifunctional cytokine that has been associated with multiple tumor types, including breast cancer (33), lung cancer (34) and ovarian cancer (35). IL-6 may promote the development of tumor types by mediating various signaling pathways, with the induction of STAT3 phosphorylation being the most common mechanism. The IL-6/STAT3 signaling transduction pathway is critical for the development and progression of malignant tumor types (36). IL6-mediated STAT3 activation may substantially upregulate the expression of a number of genes associated with tumor cell proliferation, apoptosis (BCL2 like 1, MCL1 apoptosis regulator, BCL2 family member, survivin and P53), the hypoxia response, metastasis and angiogenesis and may downregulate the
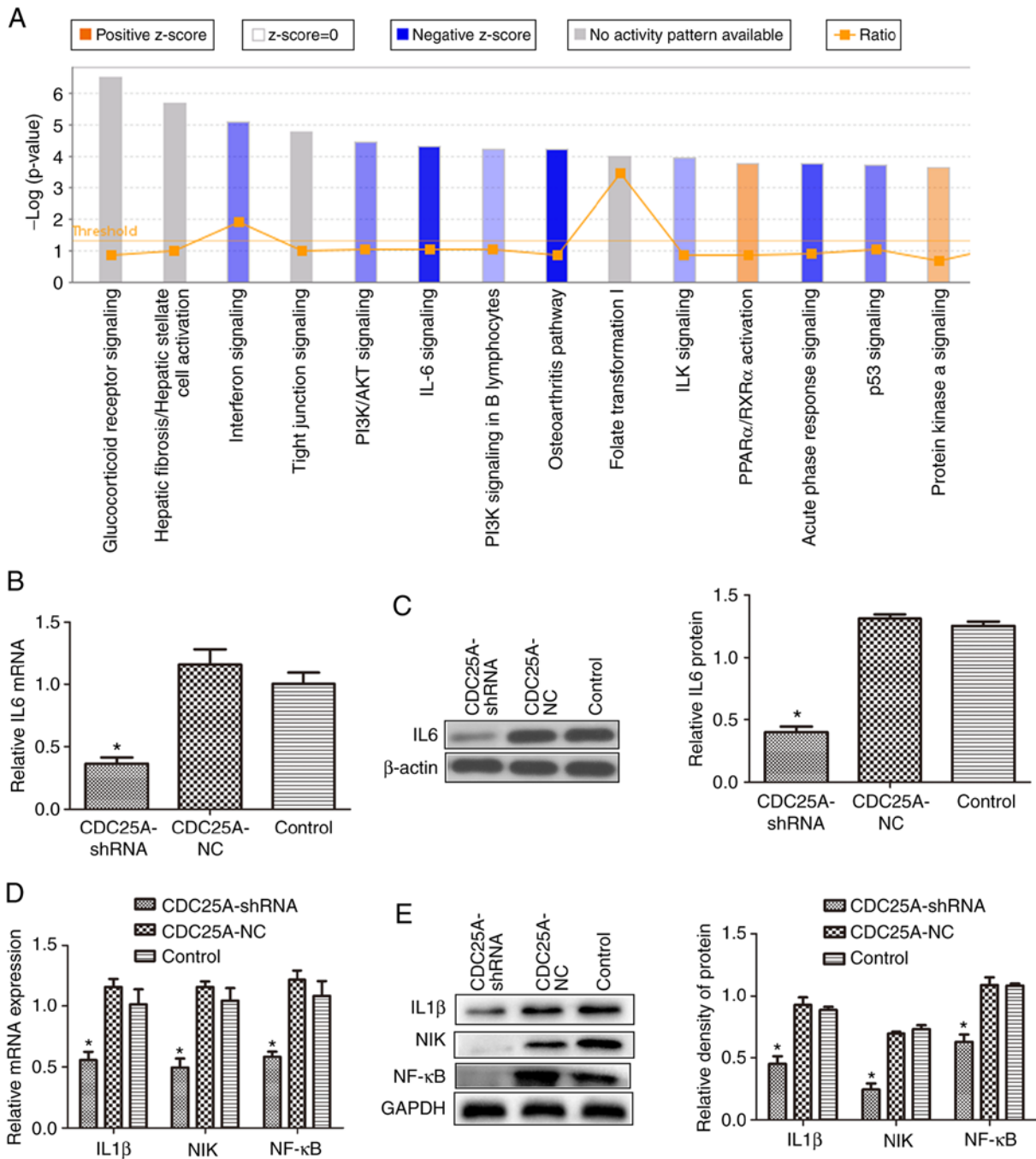
Figure 3. Classic pathway analysis and the effect of silencing CDC25A on the IL-1β/NIK/NF-κB signaling axis in HepG2 cells. (A) Classic pathway analysis results of differentially expressed genes following CDC25A expression downregulation. (B) mRNA and (C) protein levels of IL-6 in HepG2 cells were examined subsequent to the knockdown of CDC25A. (D) mRNA and (E) protein levels of IL-1β, NIK and NF-κB in HepG2 cells were examined following the knockdown of CDC25A. *P<0.05 vs. the CDC25A-NC or control group. CDC25A, cell division cycle 25A; IL, interleukin; NIK, mitogen-activated protein kinase kinase kinase kinase 4; NF-κB, nuclear factor-κB; shRNA, short hairpin RNA; NC, negative control.

expression of proapoptotic genes (37-39); this activation also serves a key function in the proliferation, apoptosis, invasion and metastasis of liver cancer cells (40,41). The present screened the differentially expressed genes in HepG2 cells with silenced CDC25A using a gene chip and revealed that the IL-6 signaling pathway was the most significantly inhibited pathway. The expression of IL-6 in HepG2 cells was confirmed to be significantly decreased subsequent to silencing the CDC25A gene (P<0.05). The same results were obtained *in vivo*, and a significant positive correlation was observed

between CDC25A and IL-6 expression in xenograft tumors (P<0.05). These results suggest that CDC25A may promote the development of liver cancer by regulating the expression of IL-6. Subsequently, the present study investigated how CDC25A regulates IL-6.

NF-κB is well known to inhibit apoptosis and promote tumor cell survival via various mechanisms. NF-κB, an important transcription factor that links inflammation and tumorigenesis, regulates the expression of various proinflammatory cytokines, including IL-6, in cancer cells and promotes

Table I. Genes with differential expression following the downregulation of cell division cycle 25A expression.

Gene symbol	Gene title	Fold change	Regulation	P-value
IL-6	Interleukin-6	-5.769	Down	<0.001
IL-1β	Interleukin-1β	-1.666	Down	<0.001
NIK	Mitogen-activated protein kinase kinase kinase kinase 4	-1.547	Down	<0.001
NF-κB	Nuclear factor-κB	-1.743	Down	<0.001
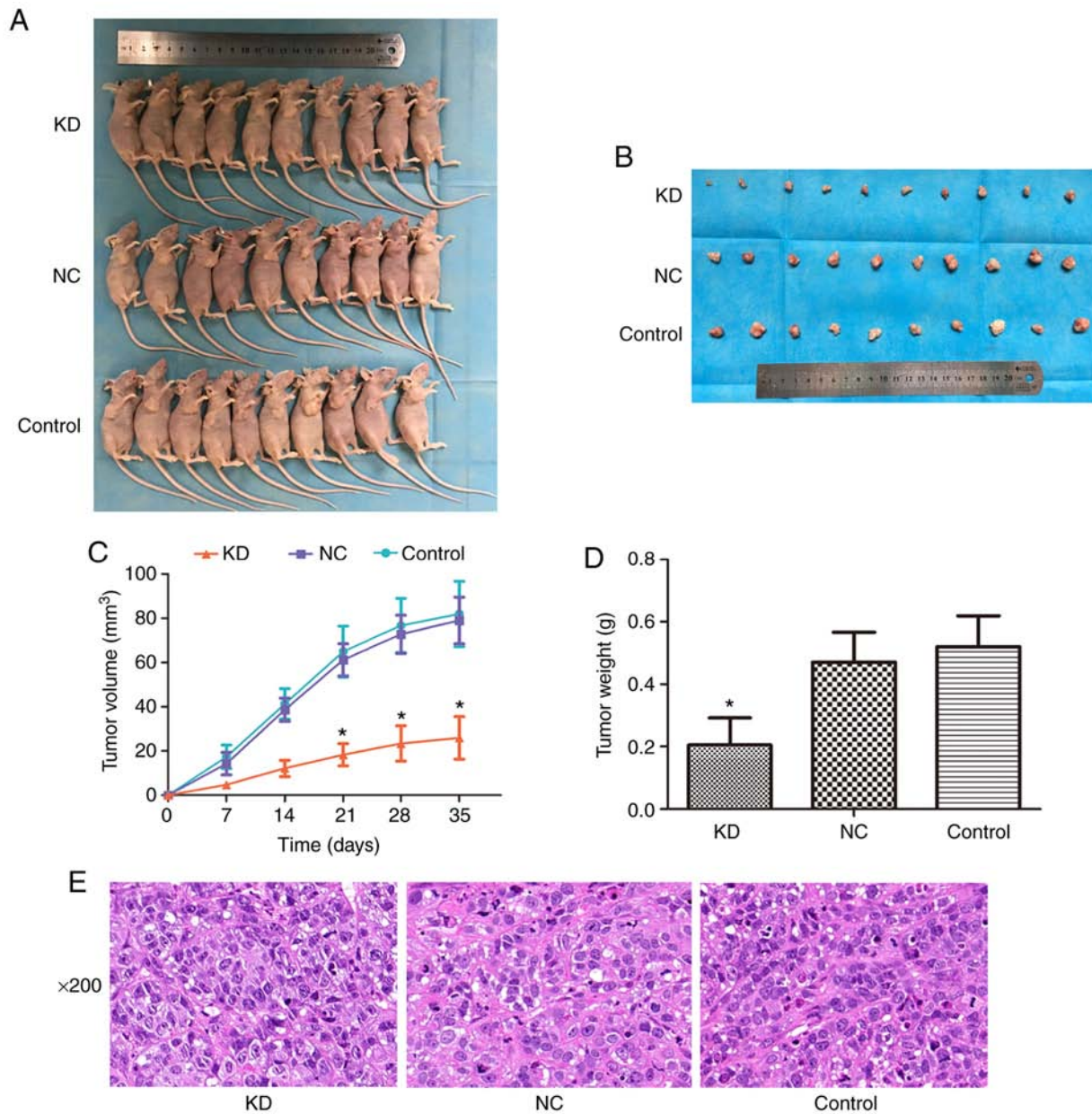
Figure 4. Effect of CDC25A downregulation on liver cancer xenograft growth. (A) Xenograft mice were sacrificed by cervical dislocation on day 35. (B) Xenograft tumors were harvested on day 35. (C) Xenograft tumor growth curve. (D) Weights of the xenograft tumors. (E) Representative haemotoxylin and eosin staining images of the xenograft tumors (magnification, x200). *P<0.05 vs. NC or control groups. CDC25A, cell division cycle 25A; KD, knockdown; NC, negative control.

tumor cell proliferation (42). Targeting the inhibition of NF-κB may downregulate the expression of IL-6 (43).

Inflammatory cytokines, including IL-1, IL-6 and IL-8, may activate the STAT3/NF-κB pathway in tumor cells, and these pathways stimulate further cytokine production, resulting in a positive feedback loop (44). IL-1β is an inflammatory factor that is involved in the NF-κB cell signaling pathway. IL-1β binds its receptor, IL-1 receptor, and exerts
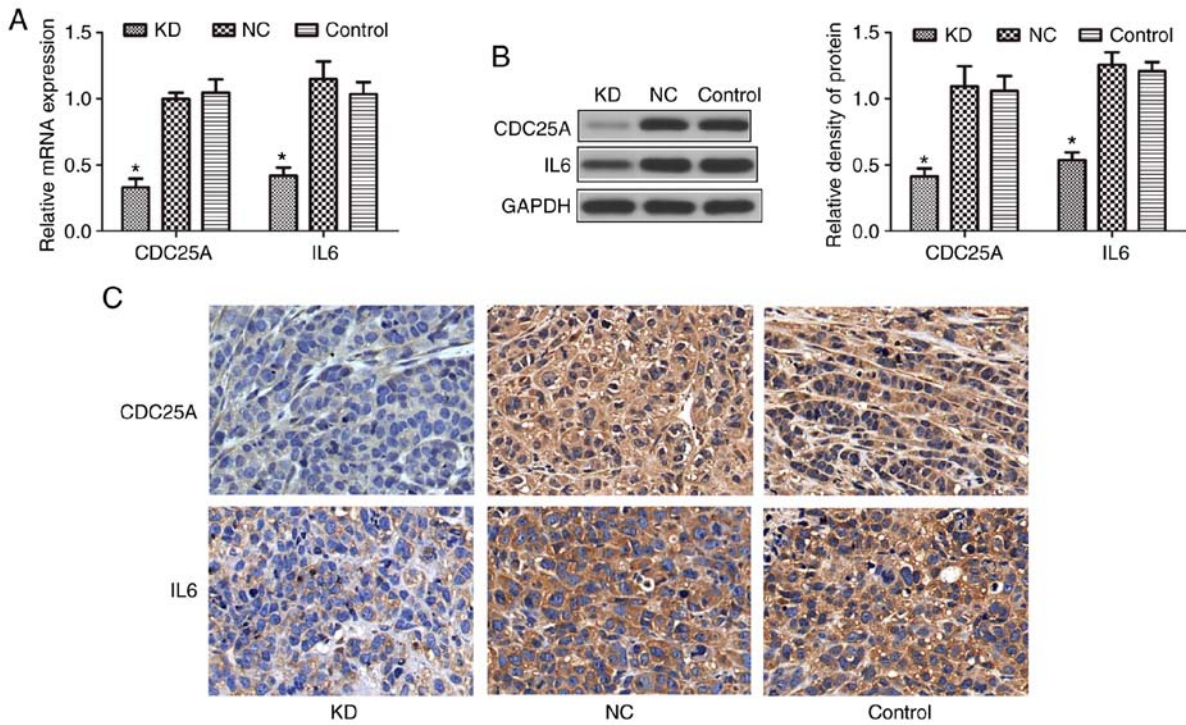
Figure 5. Association between CDC25A and IL-6. (A) mRNA and (B) protein expression levels of CDC25A and IL-6 were examined in xenograft tumors. *P<0.05 vs. NC or control groups. (C) Representative immunohistochemistry images of CDC25A and IL-6 expression in xenograft tumors (magnification, x200). CDC25A, cell division cycle 25A; IL, interleukin; KD, knockdown; NC, negative control.
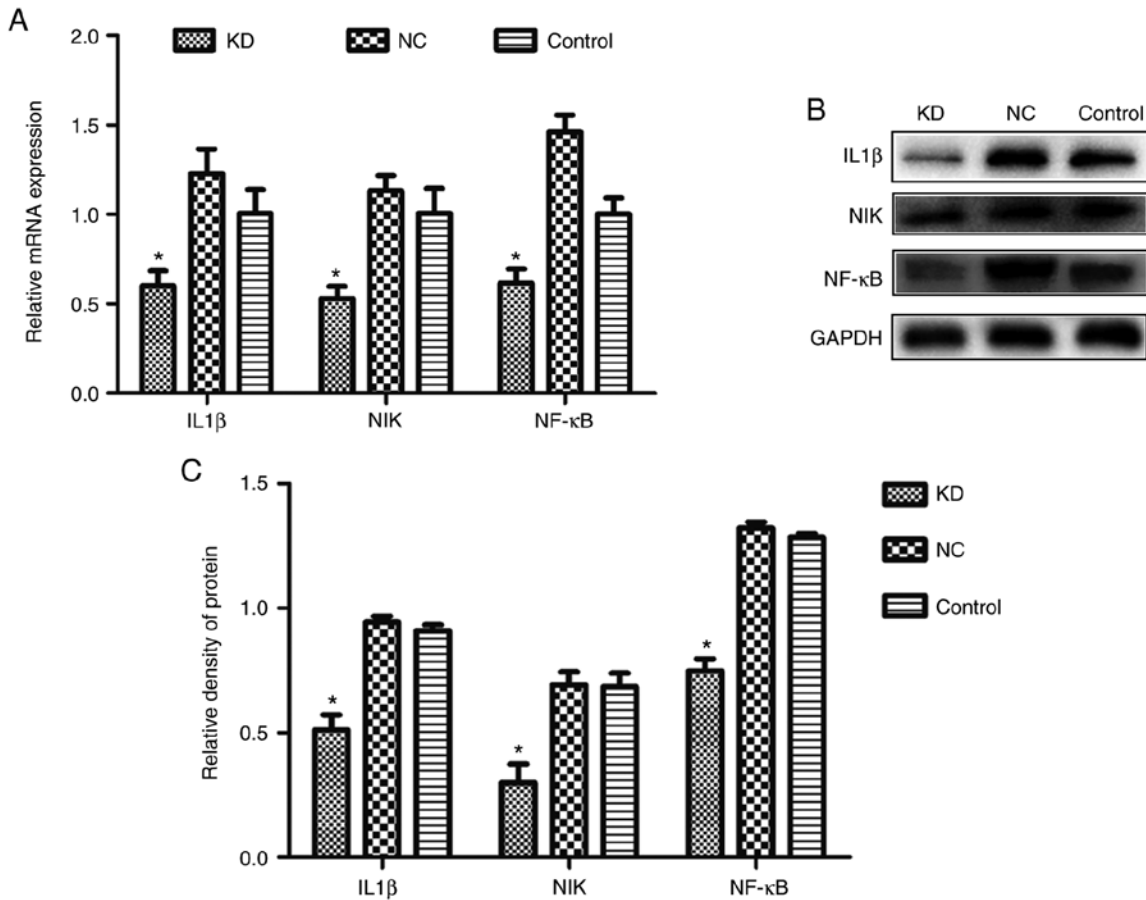

Figure 6. CDC25A affects the protein and mRNA expression levels of the IL-1β/NIK/NF-κB signaling axis in xenograft tumors. (A) Quantification of the relative expression levels of IL-1β, NIK and NF-κB mRNA in the KD, NC and control groups. (B) Representative western blot images and (C) quantification of the relative protein expression levels of IL-1β, NIK and NF-κB in three groups. *P<0.05 vs. NC or control groups. CDC25A, cell division cycle 25A; IL, interleukin; NIK, mitogen-activated protein kinase kinase kinase kinase 4; NF-κB, nuclear factor-κB; KD, knockdown; NC, negative control.

its effects on the NF-κB kinase NIK, which activates the Iκβ kinase complex and activates NF-κB (45,46). IL-1β may be induced by NF-κB activation, while IL-1β activates an autocrine signal loop that upregulates the NF-κB signal (47,48). The activated NF-κB then further promotes the expression of downstream targets IL-6 and IL-8 (49). This positive feedback loop promotes angiogenesis, tumor growth and metastasis. Gene chip analysis revealed that the IL-1β/NIK/NF-κB/IL-6 signaling axis was significantly downregulated in HepG2 cells subsequent to knocking out the CDC25A gene. The present study confirmed that the expression levels of IL-6, IL-1β, NIK and NF-κB were consistent with the chip results, and these results were also confirmed *in vivo*. Subsequent to silencing the CDC25A gene, the expression levels of IL-1β, NIK and NF-κB in the xenograft tumors were significantly decreased (P<0.05). The present study confirmed that CDC25A may regulate the expression of IL-6 by regulating the IL-1β/NIK/NF-κB signaling axis, thereby promoting the growth of liver cancer.

In summary, the present study revealed that CDC25A may positively regulate IL-6 through the IL-1β/NIK/NF-κB signaling axis, thereby promoting the proliferation and growth of liver cancer cells, and these results provide novel insight into the function and mechanism of CDC25A in liver cancer.

Availability of data and materials

All data generated or analyzed during this study are included in this published article.

Authors' contributions

JC designed and guided the experiments. SC designed and conducted the experiments, analyzed the data and drafted the manuscript. YT designed the experiments and revised the manuscript critically for important intellectual content. CY, KL and XH contributed to the analysis and interpretation of data. All authors read and approved the final manuscript.

Ethics approval and consent to participate

The present study was ethically approved by the Affiliated Tumor Hospital of Guangxi Medical University Ethics Committees (Guangxi, China).

Patient consent for publication

Not applicable.

Competing interests

The authors declare they have no competing interests.

References

1. Siegel RL, Miller KD and Jemal A: Cancer statistics 2019. CA Cancer J Clin 69: 7-34, 2019.
2. Bray F, Ferlay J, Soerjomataram I, Siegel RL, Torre LA and Jemal A: Global cancer statistics 2018: GLOBOCAN estimates of incidence and mortality worldwide for 36 cancers in 185 countries. CA Cancer J Clin 68: 394-424, 2018.
3. Yamashita T and Kaneko S: Liver cancer. Rinsho byori 64: 787-796, 2016 (In Japanese).
4. Lu X, Sun W, Tang Y, Zhu L, Li Y, Ou C, Yang C, Su J, Luo C, Hu Y and Cao J: Identification of key genes in hepatocellular carcinoma and validation of the candidate gene, cdc25a, using gene set enrichment analysis, meta-analysis and cross-species comparison. Mol Med Rep 13: 1172-1178, 2016.
5. Shen T and Huang S: The role of Cdc25A in the regulation of cell proliferation and apoptosis. Anticancer Agents Med Chem 12: 631-639, 2012.
6. Harbour JW, Luo RX, Dei Santi A, Postigo AA and Dean DC: Cdk phosphorylation triggers sequential intramolecular interactions that progressively block Rb functions as cells move through G1. Cell 98: 859-869, 1999.
7. Sur S and Agrawal DK: Phosphatases and kinases regulating CDC25 activity in the cell cycle: Clinical implications of CDC25 overexpression and potential treatment strategies. Mol Cell Biochem 416: 1-14, 2016.
8. Li H, Jiang M, Cui M, Feng G, Dong J, Li Y, Xiao H and Fan S: MiR-365 enhances the radiosensitivity of non-small cell lung cancer cells through targeting CDC25A. Biochem Biophys Res Commun 512: 392-398, 2019.
9. Qin H and Liu W: MicroRNA-99a-5p suppresses breast cancer progression and cell-cycle pathway through downregulating CDC25A. J Cell Physiol 234: 3526-3537, 2019.
10. Luo A, Zhou X, Shi X, Zhao Y, Men Y, Chang X, Chen H, Ding F, Li Y, Su D, et al: Exosome-derived miR-339-5p mediates radiosensitivity by targeting Cdc25A in locally advanced esophageal squamous cell carcinoma. Oncogene 38: 4990-5006, 2019.
11. Ataie-Kachoie P, Pourgholami MH, Richardson DR and Morris DL: Gene of the month: Interleukin 6 (IL-6). J Clin Pathol 67: 932-937, 2014.
12. Sato Y, Goto Y, Narita N and Hoon DS: Cancer cells expressing toll-like receptors and the tumor microenvironment. Cancer Microenviron 2 (Suppl 1): S205-S214, 2009.
13. Yuan FJ, Zhou YS, Wei Y, Zou C, Chen L, Huang L and Liu Z: Increased expression of IL-6 mRNA in hepatocellular carcinoma cell lines correlates with biological characteristics. Asian Pac J Cancer Prev 12: 3361-3365, 2011.
14. Schmidt-Arras D and Rose-John S: IL-6 pathway in the liver: From physiopathology to therapy. J Hepatol 64: 1403-1415, 2016.
15. Zhou M, Yang H, Learned RM, Tian H and Ling L: Non-cell-autonomous activation of IL-6/STAT3 signaling mediates FGF19-driven hepatocarcinogenesis. Nat Commun 8: 15433, 2017.
16. Rayet B and Gelinas C: Aberrant rel/nfkb genes and activity in human cancer. Oncogene 18: 6938-6947, 1999.
17. Yin L and Yu X: Arsenic-induced apoptosis in the p53-proficient and p53-deficient cells through differential modulation of NFkB pathway. Food Chem Toxicol 118: 849-860, 2018.
18. Sheng ML, Xu GL, Zhang CH, Jia WD, Ren WH, Liu WB, Zhou T, Wang YC, Lu ZL, Liu WF, et al: Aberrant estrogen receptor alpha expression correlates with hepatocellular carcinoma metastasis and its mechanisms. Hepatogastroenterology 61: 146-150, 2014.
19. Xu H, Wei Y, Zhang Y, Xu Y, Li F, Liu J, Zhang W, Han X, Tan R and Shen P: Oestrogen attenuates tumour progression in hepatocellular carcinoma. J Pathol 228: 216-229, 2012.
20. Hoesel B and Schmid JA: The complexity of NF-κB signaling in inflammation and cancer. Mol Cancer 12: 86, 2013.

21. Hong HY, Choi J, Cho YW and Kim BC: Cdc25A promotes cell survival by stimulating NF-κB activity through IκB-α phosphorylation and destabilization. Biochem Biophys Res Commun 420: 293-296, 2012.
22. He P: Screening of differentially expressed genes in liver cancer HepG2 cells after silencing CDC25A gene. Guangxi Med Univ, 2018.
23. Livak KJ and Schmittgen TD: Analysis of relative gene expression data using real-time quantitative PCR and the 2(-Delta Delta C(T)) method. Methods 25: 402-408, 2001.
24. Källström H, Lindqvist A, Pospisil V, Lundgren A and Rosenthal CK: Cdc25A localisation and shuttling: Characterisation of sequences mediating nuclear export and import. Exp Cell Res 303: 89-100, 2005.
25. Dozier C, Mazzolini L, Cénac C, Froment C, Burlet-Schiltz O, Besson A and Manenti S: CyclinD-CDK4/6 complexes phosphorylate CDC25A and regulate its stability. Oncogene 36: 3781-3788, 2017.
26. Wang Z, Kar S and Carr BI: Cdc25A protein phosphatase: A therapeutic target for liver cancer therapies. Anticancer Agents Med Chem 8: 863-871, 2008.
27. Zou X, Tsutsui T, Ray D, Blomquist JF, Ichijo H, Ucker DS and Kiyokawa H: The cell cycle-regulatory CDC25A phosphatase inhibits apoptosis signal-regulating kinase 1. Mol Cell Biol 21: 4818-4828, 2001.
28. Liang J, Cao R, Zhang Y, Xia Y, Zheng Y, Li X, Wang L, Yang W and Lu Z: PKM2 dephosphorylation by Cdc25A promotes the Warburg effect and tumorigenesis. Nat Commun 7: 12431, 2016.
29. Feng X, Wu Z, Wu Y, Hankey W, Prior TW, Li L, Ganju RK, Shen R and Zou X: Cdc25A regulates matrix metalloprotease 1 through Foxo1 and mediates metastasis of breast cancer cells. Mol Cell Biol 31: 3457-3471, 2011.
30. Wang XQ, Zhu YQ, Lui KS, Cai Q, Lu P and Poon RT: Aberrant Polo-like kinase 1-Cdc25A pathway in metastatic hepatocellular carcinoma. Clin Cancer Res 14: 6813-6820, 2008.
31. Xu X, Yamamoto H, Sakon M, Yasui M, Ngan CY, Fukunaga H, Morita T, Ogawa M, Nagano, H, Nakamori S, *et al*: Overexpression of CDC25A phosphatase is associated with hypergrowth activity and poor prognosis of human hepatocellular carcinomas. Clin Cancer Res 9: 1764-1772, 2003.
32. Xu X, Yamamoto H, Liu G, Ito Y, Ngan CY, Kondo M, Nagano H, Dono K, Sekimoto M and Monden M: CDC25A inhibition suppresses the growth and invasion of human hepatocellular carcinoma cells. Int J Mol Med 21: 145-152, 2008.
33. Fu S and Lin J: Blocking interleukin-6 and interleukin-8 signaling inhibits cell viability, colony-forming activity, and cell migration in human triple-negative breast cancer and pancreatic cancer cells. Anticancer Res 38: 6271-6279, 2018.
34. Huang Q, Zhang Z, Liao Y, Liu C, Fan S, Wei X, Ai B and Xiong J: 17β-estradiol upregulates IL6 expression through the ERβ pathway to promote lung adenocarcinoma progression. J Exp Clin Cancer Res 37: 133, 2018.
35. Wang Y, Zong X, Mitra S, Mitra AK, Matei D and Nephew KP: IL-6 mediates platinum-induced enrichment of ovarian cancer stem cells. JCI Insight 3: pii: 122360, 2018.
36. Yin Z, Ma T, Lin Y, Lu X, Zhang C, Chen S and Jian Z: IL-6/STAT3 pathway intermediates M1/M2 macrophage polarization during the development of hepatocellular carcinoma. J Cell Biochem 119: 9419-9432, 2018.
37. Bournazou E and Bromberg J: Targeting the tumor microenvironment: JAK-STAT3 signaling. JAKSTAT 2: e23828, 2013.
38. Rokavec M, Wu W and Luo JL: IL6-mediated suppression of miR-200c directs constitutive activation of inflammatory signaling circuit driving transformation and tumorigenesis. Mol Cell 45: 777-789, 2012.
39. Al Zaid Siddiquee K and Turkson J: STAT3 as a target for inducing apoptosis in solid and hematological tumors. Cell Res 18: 254-267, 2008.
40. Subramaniam A, Shanmugam MK, Ong TH, Li F, Perumal E, Chen L, Vali S, Abbasi T, Kapoor S, Ahn KS, *et al*: Emodin inhibits growth and induces apoptosis in an orthotopic hepatocellular carcinoma model by blocking activation of STAT3. Br J Pharmacol 170: 807-821, 2013.
41. Ma H, Yan D, Wang Y, Shi W, Liu T, Zhao C, Huo S, Duan J, Tao J, Zhai M, *et al*: Bazedoxifene exhibits growth suppressive activity by targeting interleukin-6/glycoprotein 130/signal transducer and activator of transcription 3 signaling in hepatocellular carcinoma. Cancer Sci 110: 950-961, 2019.
42. Xiang M, Birkbak NJ, Vafaizadeh V, Walker SR, Yeh JE, Liu S, Kroll Y, Boldin M, Taganov K, Groner B, *et al*: STAT3 induction of miR-146b forms a feedback loop to inhibit the NF-κB to IL-6 signaling axis and STAT3-driven cancer phenotypes. Sci Signal 7: ra11, 2014.
43. Duan XH, Li H, Han XW, Ren JZ, Li FY, Ju SG, Chen PF and Kuang DL: Upregulation of IL-6 is involved in moderate hyperthermia induced proliferation and invasion of hepatocellular carcinoma cells. Eur J Pharmacol 833: 230-236, 2018.
44. Korkaya H, Liu S and Wicha MS: Regulation of cancer stem cells by cytokine networks: Attacking cancer's inflammatory roots. Clin Cancer Res 17: 6125-6129, 2011.
45. Stylianou E and Saklatvala J: Interleukin-1. Int J Biochem Cell Biol 30: 1075-1079, 1998.
46. Wu R, Chen B, Jia X, Qiu Y, Liu M, Huang C, Feng J and Wu Q: Interleukin-1β influences functional regeneration following nerve injury in mice through nuclear factor-κB signaling pathway. Immunology 156: 235-248, 2019.
47. Sun K, Xu L, Jing Y, Jing Y, Han Z, Chen X, Cai C, Zhao P, Zhao X and Yang L: Autophagy-deficient Kupffer cells promote tumorigenesis by enhancing mtROS-NF-κB-IL1α/β-dependent inflammation and fibrosis during the preneoplastic stage of hepatocarcinogenesis. Cancer Lett 388: 198-207, 2017.
48. Nomura A, Gupta VK, Dauer P, Sharma NS, Dudeja V, Merchant N, Saluja AK and Banerjee S: NFκB-mediated invasiveness in CD133+ pancreatic TICs is regulated by autocrine and paracrine activation of IL1 signaling. Mol Cancer Res 16: 162-172, 2018.
49. Voronov E, Shouval DS, Krelin Y, Cagnano E, Benharroch D, Iwakura Y, Dinarello CA and Apte RN: IL-1 is required for tumor invasiveness and angiogenesis. Proc Natl Acad Sci USA 100: 2645-2650, 2003.